Title: Organometallic Derivatization of the Nematocidal Drug Monepantel Leads to Promising Antiparasitic Drug Candidates

Authors: Jeannine Hess; Malay Patra; Loganathan Rangasamy; Sandro Konatschnig; Olivier Blacque; Abdul Jabbar; Patrick Mac; Erik M. Jorgensen; Robin B. Gasser; Gilles Gasser, Ph.D

To be cited as: 10.1002/chem.201602851

Link to VoR: https://doi.org/10.1002/chem.201602851

Organometallic Derivatization of the Nematocidal Drug Monepantel Leads to Promising Antiparasitic Drug Candidates

Jeannine Hess,[a] Malay Patra,[a] Loganathan Rangasamy,[a] Sandro Konatschnig,[a] Olivier Blacque,[a] Abdul Jabbar,[b] Patrick Mac,[c] Erik M. Jorgensen,[c] Robin B. Gasser[b,] and Gilles Gasser[a,*]*

[a] Department of Chemistry, University of Zurich, Winterthurerstrasse 190, CH-8057 Zurich, Switzerland

[b] Faculty of Veterinary and Agricultural Sciences, The University of Melbourne, Parkville, Victoria 3010, Australia

[c] Howard Hughes Medical Institute, Department of Biology, University of Utah, Salt Lake City, UT 84112-0840, USA

* Corresponding authors: Email: robinbg@unimelb.edu.au; WWW: http://www.gasserlab.org/; Tel. +61 3 9731 2283; Email: gilles.gasser@chem.uzh.ch; WWW: www.gassergroup.com; Tel.: +41 44 635 46 30;

Abbreviations: AADs – Amino-Acetonitrile Derivatives; *Caenorhabditis elegans* – *C. elegans*; *C. felis* – *Ctenocephalides felis*; *D. immitis* – *Dirofilaria immitis*; ESI-MS – Electrospray Ionization-Mass Spectrometry; *H. contortus* – *Haemonchus contortus;* H2DCFDA – 2′,7′-dichlorofluorescein diacetate; LDA – larval development assay; *L. cuprina* – *Lucilia cuprina*; *m*-CPBA – *meta*-chloroperoxybenzoic acid; nAChR – nicotinic acetylcholine receptor; o.n. – overnight; *P. falciparum* – *Plasmodium falciparum*; ROS – reactive oxygen species; *R. sanguineus* – *Rhipicephalus sanguineus;* r.t. – room temperature; SAR – Structure Activity Relationship; TBH – *tert*-Butyl hydroperoxide; *T. colubriformis* – *Trychostrongylus colubriformis.*

Abstract

The discovery of novel drugs against animal parasites is in high demand due to drug resistance problems encountered by farmers around the world. In this study, we describe the synthesis and characterization of 27 organic and organometallic derivatives of the recently launched nematocidal drug monepantel (Zolvix®). The compounds were isolated as racemates and were characterized by ^{1}H, ^{13}C and ^{19}F NMR spectroscopies, mass spectrometry, and IR spectroscopy, and their purity was verified by microanalysis. The molecular structures of 9 compounds were confirmed by X-ray crystallography. The anthelmintic activity of the newly designed analogues was evaluated *in vitro* against the economically important parasites *Haemonchus contortus* and *Trichostrongylus colubriformis*. Moderate nematocidal activity was observed for 9 of the 27 compounds. The activity is accounted for by activation of a known monepantel target, the ACR-23 ion channel. Production of reactive oxygen species (ROS) may confer a secondary activity to the organometallic analogues. Two compounds, an organic precursor (**3a)** and a cymantrene analogue (**9a**), had activities against microfilariae of *Dirofilaria immitis* in the low μg/mL range.

Introduction

Multicellular parasites including roundworms (nematodes), flatworms (trematodes and cestodes) and arthropods (e.g., fleas, flies and ticks) cause morbidity and mortality in animals worldwide,[1] resulting in a substantial loss to global food production annually.[1b, 1g] The control of parasites relies largely on the use of anti-parasitic drugs.[2] However, drug resistance is now quite widespread.[1a, 3] Therefore, the development of new drugs or chemical modifications of existing drugs are crucial to ensure sustainable chemical control of parasites in the future.

In this context, the discovery of a structurally new amino-acetonitrile class of synthetic anti-parasitic compounds (AADs, see Figure 1) by Novartis Animal Health in 2008 was a major breakthrough.[4] An extensive structure-activity relationship (SAR) study resulted in the development of monepantel (AAD 1566, Figure 1), which was released under the trade name Zolvix® in 2009 for the treatment of nematode infections in sheep.[5]

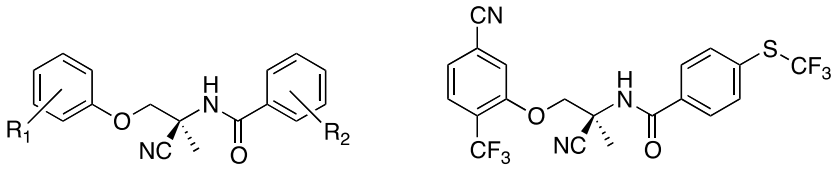

Amino-acetonitrile derivatives (AADs)

AAD 1566 (Monepantel)

Figure 1. General structure of Amino-Acetonitrile Derivatives (AADs) and monepantel (AAD 1566).

Monepantel targets ligand-gated ion channels in the nematode-specific DEG-3 family.[4] These channels are related to nicotinic acetylcholine receptors, but they are gated by betaine and choline rather than acetylcholine.[6] Monepantel acts on MPTL-1 receptors in *Haemonchus contortus* (*H. contortus*) and the homologs ACR-20 and ACR-23 in the free-living model nematode *Caenorhabditis elegans* (*C. elegans*) The drug acts as a positive allosteric modulator, hyperactivating these channels.[6c, 7] An *in vitro* selection procedure by Rufener *et al.* revealed that monepantel resistance in *H. contortus* can develop relatively rapidly by a single loss-of-function mutation. Indeed, monepantel-resistant worms in livestock were reported within a few years.[3d, 3e, 8]

It is of increasing importance to search for structurally or functionally unique classes of compounds to control parasites.[3a] To date, this quest has been focused mainly on organic compounds, but metal-based compounds have had impressive success in other fields of medicinal chemistry.[9] Specifically, recent efforts have identified anti-cancer,[10] -malarial,[11] -trypanosomal,[12] -bacterial[13] and -schistosomal[14] compounds. A particular class of metal compounds, namely organometallic complexes (i.e. compounds with at least one direct metal-carbon bond), has also shown great promise as an anti-infective.[13, 15] Ferroquine, the ferrocenyl analogue of the antimalarial drug chloroquine, is the most prominent example of an organometallic drug candidate used against parasites. The introduction of a ferrocenyl moiety alters the mode of action of the parent drug and renders it active against chloroquine-resistant *Plasmodium falciparum* (*P. falciparum*) strains.[11a] Similarly, an altered mode of action was evident in the ferrocenyl derivative of the anticancer drug tamoxifen, named ferrocifen. While tamoxifen is only active against estrogen (+) breast cancers, ferrocifen is active against both estrogen (+) and estrogen (–) cancers.[16] To the best of our knowledge, reports of nematocidal organometallic complexes are rare.[17]

With the aim of developing new classes of nematocidal drugs, we recently initiated a program to design and test organometallic analogues of the organic anthelmintic monepantel. The aryloxy unit of the original molecule was substituted with sandwich (ferrocene, ruthenocene) and half-sandwich (cymantrene) organometallic moieties in order to introduce metal specific modes of action as well as with various organic moieties. The functional groups at the benzamide unit of the organometallic and organic analogue were further varied (SCF_3, OCF_3, CF_3, F, Cl, Br, I etc.). Presence of different functional groups are expected to modulate the lipophilicity, biodistribution and pharmacokinetic properties, thereby influencing the biological properties of the newly designed monepantel analogues. These modifications resulted in a library of 27 organic/organometallic derivatives of monepantel for structure-activity relationship study. The initial biological screenings reported here demonstrate that some of the compounds retain activity against monepantel targets, while gaining novel properties, such as the production of reactive oxidative species (ROS). Additionally, we demonstrate, for the first time, that AADs, including our organic and organometallic analogues, possess activity against *Dirofilaria immitis* (*D. immitis*) microfilariae.

Results and Discussion

Design of organometallic analogues

Monepantel consists of an aryloxy and a benzamide unit connected by a chiral C2 spacer. Preliminary metabolism studies indicated that the benzamide unit plays a crucial role in the *in vivo* activity of monepantel.[18] Therefore, with the intention to keep the benzamide part in place, we designed our first organometallic monepantel analogues by replacing the aryloxy part of monepantel with a ferrocenyl unit (Scheme 1). The ferrocene/ferrocenium system has redox properties favorable for production of ROS, which can improve toxicity as shown for ferroquine and ferrocifen.[11b, 19] Subsequently, we employed two different strategies to study the structure activity relationship (SAR) of monepantel analogues. In Strategy I a series of organic and organometallic derivatives were synthesized in which the functional group at the 4-position of the benzamide moiety was varied (Strategy I, Scheme 1). In Strategy II (Scheme 1), we designed organic and organometallic derivatives of **5a** in order to evaluate the importance of the organometallic moiety. For this purpose, the ferrocenyl subunit was swapped with two different organometallic moieties, namely ruthenocene and cymantrene. Replacing the Fe(II) core with a comparatively inert Ru(II) center may allow us to probe the relevance of Fe(II)/Fe(III)-mediated redox activity of the compound. By contrast to ferrocene and ruthenocene, cymantrene conjugates of organic drugs are rarely studied for their anti-parasitic potency.[20] The metal center in cymantrene is isoelectronic to that of ferrocene and the two metallocenes are nearly isosteric. However, they have different redox behavior and the metal centers are in +1 and +2 oxidation states in cymantrene and ferrocene, respectively. Therefore, comparison of these metallocenyl analogues should illuminate any metal-mediated modes of action of our compounds.

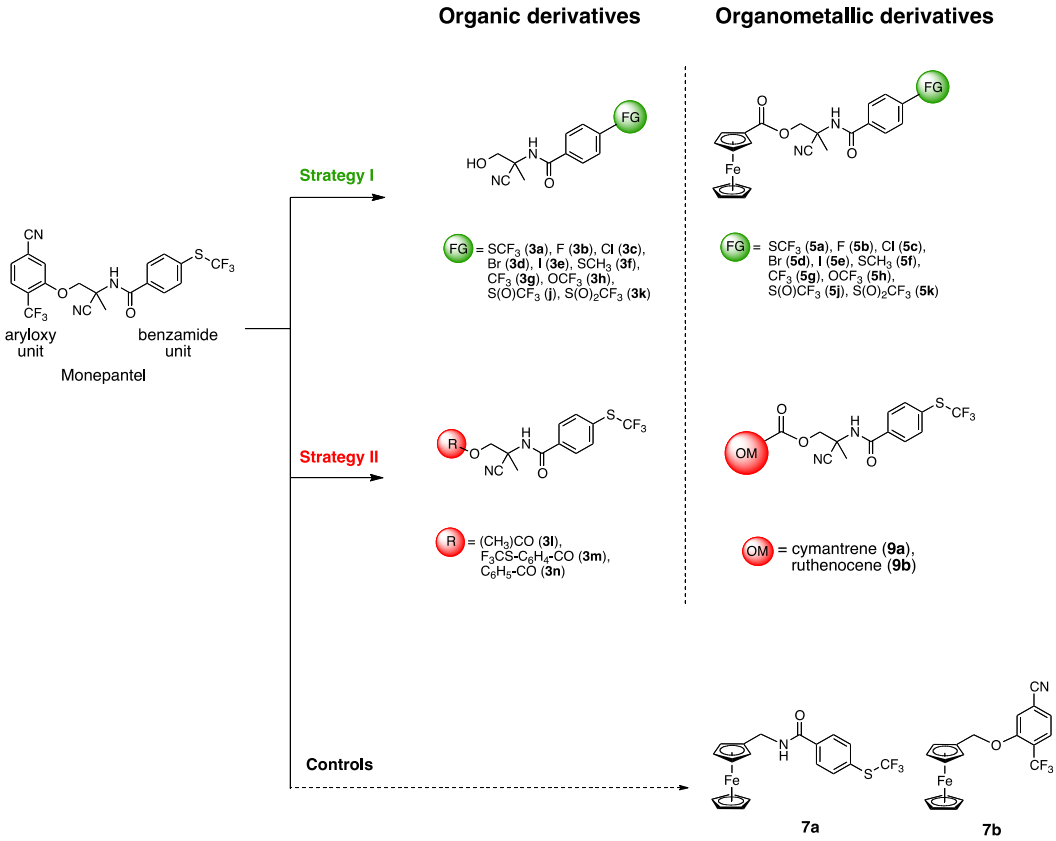

Scheme 1. Schematic presentation of the design of organometallic derivatives based on the lead structure of AAD 1566 (monepantel).

Synthesis and Characterization

Organometallic analogues **5a**-**5h** were prepared in a two-step procedure as outlined in Scheme 2. The central core, 2-amino-2-hydroxymethylproprionitrile (**1**), was synthesized following the procedure described by Gauvry *et al.*[21] In a subsequent reaction, the amide bond between **1** and the commercially available compounds **2a** – **2h** bearing a chlorocarbonyl moiety was formed. Initially, we attempted to synthesize **3a**, following the procedure of Gauvry *et al.*[21] However, instead of the desired compound, two different products, namely 2-cyano-2-(4 ((trifluoromethyl)thio)benzamido)propyl acetate (**3l**) and 2-cyano-2-(4-((trifluoromethyl)thio)benzamido)propyl 4-((trifluoromethyl)thio)benzoate (**3m**) were isolated with yields of 21% and 3%, respectively (Scheme 2). Therefore, we improved the protocol by changing the base from sodium hydroxide to triethylamine, which resulted in the formation of the desired **3a** with a yield of 74%. Following the same procedure, compounds **3b** – **3h** were isolated in moderate to good yields. **3a** was further reacted with benzoyl chloride under basic conditions and compound **3n** was

obtained at an 86% yield. Finally, esterification of **3a – 3h** with ferrocenecarboxylic acid (**4**) yielded the desired compounds **5a – 5h** as yellow or orange solids. Although it was shown that the efficacy of AADs against nematodes is enantio-selective, we decided to perform the synthesis and biological evaluation with the organometallic racemates (**5a – 5h**). Lower potency is expected from evaluating racemic mixtures rather than enantio-pure compounds, but this approach provided an initial estimation of potency.

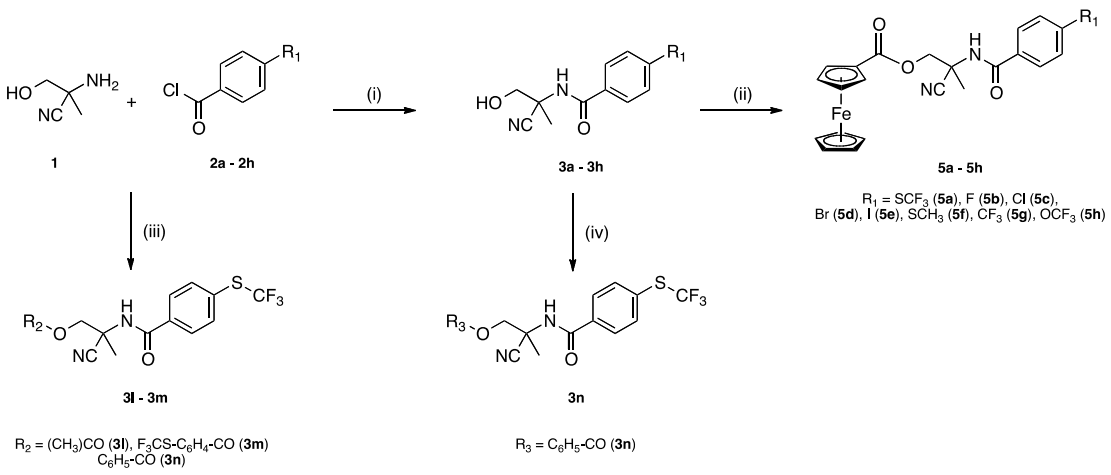

Scheme 2. Reagents and conditions: (i) NEt_3, dry CH_2Cl_2, 1.5 h – 24 h, r.t., 26% - 74%. (ii) a) ferrocenecarboxylic acid (**4**), oxalyl chloride, dry CH_2Cl_2, r.t.; b) NEt_3, dry CH_2Cl_2, o.n., r.t., 25% - 94% after two steps; (iii) 4-(trifluoromethylthio)benzoyl chloride, dry ethyl acetate, 1M NaOH, 3 h, r.t., 21% (**3l**) and 3% (**3m**). (iv) benzoyl chloride, NEt_3, dry CH_2Cl_2, 2 h, r.t. 86% (**3n**).

Monepantel is rapidly metabolized *in vivo* to the sulfone derivative, with the corresponding sulfoxide as an intermediate.[18, 22] Because these are active metabolites,[22] we synthesized the sulfone and sulfoxide derivatives of **5a** (**5j** and **5k**, Scheme 3). For this purpose, the SCF_3 functionality of **3a** was selectively oxidized using different equivalents of *meta*-chloroperoxybenzoic acid (*m*-CPBA) at –78 °C. The resulting organic precursors **3j** and **3k** were isolated as colourless solids in moderate yields. An esterification of **3j** or **3k** with **4** yielded the final ferrocenyl-based sulfoxide and sulfone derivatives, 2-cyano-2-(4-((trifluoromethyl)sulfinyl)benzamido)propyl ferroceneoate (**5j**) and 2-cyano-2-4-((trifluoromethyl)sulfonyl)benzamido)propyl ferroceneoate (**5k**) (Scheme 3).

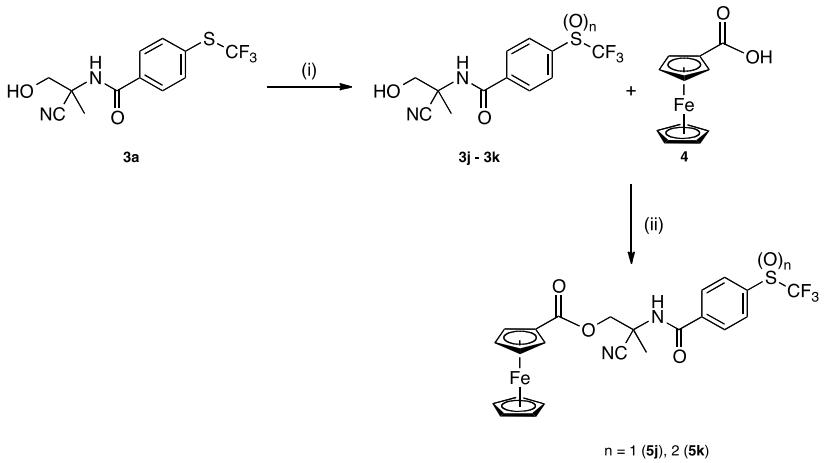

Scheme 3. Reagents and conditions: (i) *m*-CPBA, dry CH_2Cl_2, -78 °C→r.t., 45% (**3j**) and 43% (**3k**). (ii) a) oxalyl chloride, dry CH_2Cl_2, r.t.; b) NEt_3, dry CH_2Cl_2, o.n., r.t., 70% (**5j**) and 87% (**5k**) over two steps.

The ferrocenyl moiety of **5a** was replaced with two different organometallic moieties to assess their effect on the anthelmintic activity. In contrast to the ferrocenyl derivative **5a**, the cymantrene derivative **9a** and ruthenocene derivative **9b** (Scheme 4) are not expected to produce ROS. **9a** and **9b** were synthesized following the synthetic pathway outlined in Scheme 5. Initially, cymantrene carboxylic acid (**8a**) and ruthenocenyl carboxylic acid (**8b**) were synthesized according to published procedures.[23] While **8a** was linked to **3a** using the one-step Steglich esterification reaction, **8b** required activation with oxalyl chloride and then reaction with **3a**.

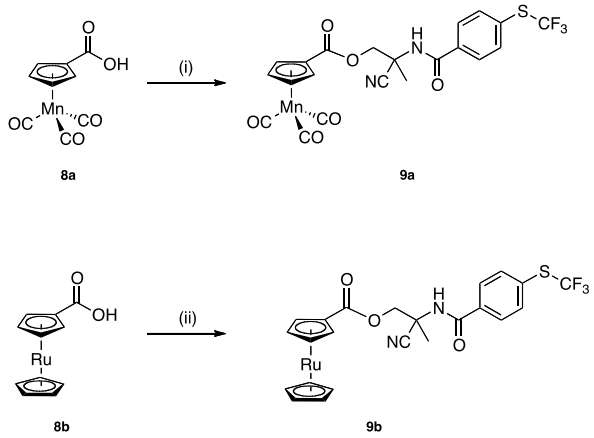

Scheme 4. Reagents and conditions: (i) **3a**, DCC, DMAP, dry Et_2O/CH_2Cl_2, 24 h, 0 °C→r.t., 74%; (ii) a) oxalyl chloride, dry CH_2Cl_2; b) **3a**, NEt_3, dry CH_2Cl_2, r.t., o.n., 41% after two steps.

In order to assess the importance of the chiral C2 spacer between the aryloxy and the benzamide unit, two additional organometallic derivatives (**7a** and **7b**) were synthesized. **7a** and **7b** contain the benzamide and the aryloxy units, respectively, which are connected to a ferrocenyl moiety *via* an amide or an ether functionality, rather than the C2 spacer (Scheme 1). The organometallic precursors ferrocenylmethylamine (**6a**) and hydroxymethylferrocene (**6b**) were synthesized following published procedures.[24] **7a** was then readily prepared by amide bond formation of **6a** with commercially available 4-(trifluoromethylthio)benzoyl chloride under alkaline conditions and *N*-ferrocenyl-4-((trifluoromethyl)thio)benzamide (**7a**) was isolated as a bright yellow solid. 3-(ferrocenyloxy)-4-(trifluoromethyl)benzonitrile (**7b**) was isolated after an aromatic nucleophilic substitution reaction with the ferrocenyl alcohol (Scheme 5).

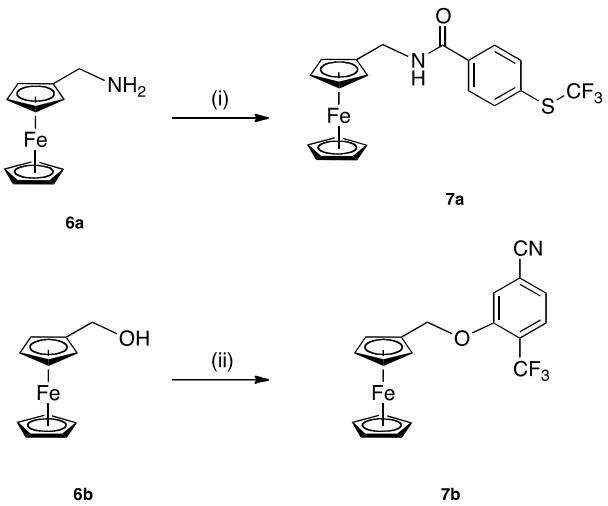

Scheme 5. Reagents and conditions: (i) 4-(trifluoromethylthio)benzoyl chloride, NEt_3, dry THF, 16 h, r.t., 32%; (ii) 3-fluoro-4-(trifluoromethyl)benzonitrile, NaH, dry THF, 0 °C→r.t., 36 h, 16%.

All novel compounds were unambiguously characterized by ^{1}H, ^{13}C, and ^{19}F NMR spectroscopy, mass spectrometry, and IR spectroscopy, and their purities were verified by elemental analysis (see Experimental Section and SI for further details). The ^{13}C NMR spectra of the compounds containing a fluorine atom (**3a**, **3b**, **3g**, **3h**, **3j**, **3k**, **3l**, **3m**, **3n**, **5a**, **5b**, **5g**, **5h**, **5j**, **5k**, **7a**, **7b**, **9a** and **9b**) showed a characteristic coupling to the adjacent carbon atom resulting in a quadruplet splitting pattern. Most of the derivatives were detected mainly as their $[M+H]^+$ species by ESI-mass spectrometry (positive detection mode) with traces of $[M+Na]^+$ and $[M+K]^+$ species present.

X-ray crystallography

The structures of complexes **3a**, **3b**, **3f**, **3g**, **5a, 5c**, **5d**, **5h**, and **5k** have been further corroborated by single crystal X-ray diffraction studies. Example structures of **3f** and **5d** are shown in Figure 2 (see Figures S1 – S3 in SI for the other structures). The X-ray diffraction studies confirmed the formation of the amide bond between the 2-amino-2-hydroxymethylproprionitrile species **1** and the substituted compounds **2a** – **2h** through the carbonyl group to form the monepantel analogues. The reported crystal structure of monepantel possesses four crystallographically independent molecules of the (*S*)-enantiomer, which only differ from each other by the orientation

of the terminal SCF_3 group relative to the rest of the molecule.[5] The central part of the monepantel enantiomer exhibits a *Z*-type conformation between the chiral carbon atom C* and the carbonyl oxygen atom (on the same side of the central C–N bond), together with an *E*-type conformation between the carbonyl carbon atom and the methyl group (on opposite sides of the N–C* bond) along the (O=)C-N(H)-C*-CH_3 moiety. Indeed, the O-C-N-C* torsional angles in the independent molecules are observed close to 0° (*Z*-type), between 1.9(5) and 5.7(5)°. That very narrow range was expected because of the pronounced double-bond character of the central bond, due to electron delocalization with the carbonyl group (as revealed by relatively short C–N bond distances in the range 1.355(4) – 1.366(5) Å). Despite the single-bond character of the N–C* bond (1.452(6) – 1.462(5) Å), the C-N-C*-C torsional angles also fall in a narrow range close to 180° (*E*-type; 165.4(4) – 169.0(4)°).

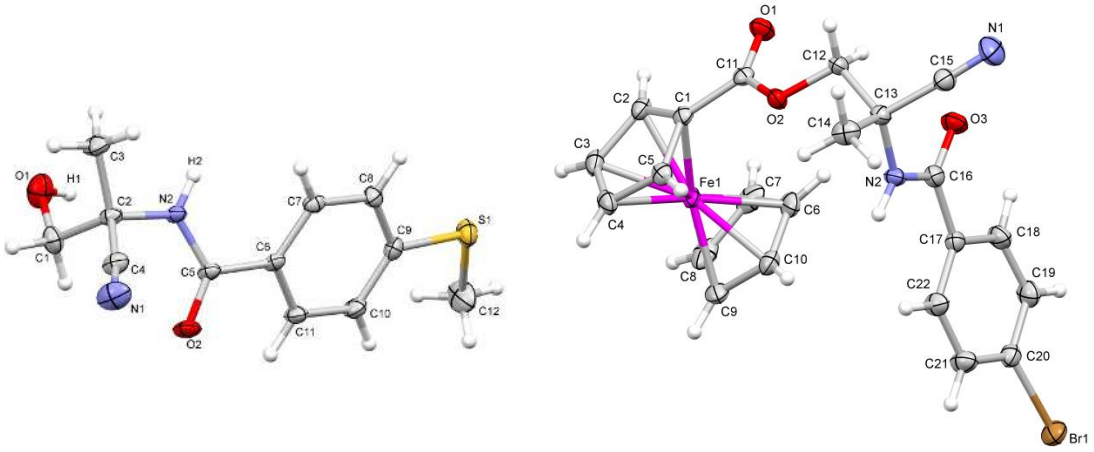

Figure 2. Molecular structure of compounds **3f** (left) and **5d** (right) with an atomic numbering scheme.

The *Z*-type conformation is observed in all our new amino-acetonitrile derivatives. The largest O-C-N-C* torsional angle was found in the crystal structure of **3a** with a value as small as 8.6(2)°. More interestingly, the *E*-type conformation is also generally observed in our compounds: all C-N-C*-C torsional angles fall in the range 160.4(3) – 179.0(1)° except for **3a** with 72.9(2)°, 62.0(2)° and **5k** 59(2)/68.0(6)° (two-components disorder), respectively. The crystal structures of **5c**, **5d**, **5f**, **5g** and **5k** confirmed the coordination of the organic species on a ferrocenyl moiety to form a carboxylic function. The CO_2 fragment is essentially coplanar with the five-

membered ring, and the C–C bond between the ring and the carboxyl falls in the normal range for a single $Csp^2 – Csp^2$ bond (from 1.459(2) Å for **5k** to 1.484(6) Å for **5f**). The relative orientation of the rest of the molecule with the ferrocenyl moiety mainly depends on the intermolecular interactions which link the molecules in the solid state, mainly C-H···O, C-H···N and N-H···O hydrogen bonds as observed in the crystal structures of the organic molecules **3a**, **3b**, **3f** and **3g**. All compounds except **3g** crystallized in triclinic, monoclinic or orthorhombic centrosymmetric space groups, which indicates the presence of both (*R*) and (*S*) enantiomers (racemates) in the crystals. **3g** crystallized in a racemic crystal structure as well, but in the non-centrosymmetric space group $Pna2_1$, with two crystallographically independent (*S*) and (*R*) enantiomer molecules in the asymmetric unit in a 1:1 ratio.

Activity against *H. contortus* and *T. colubriformis*

H. contortus and *Trychostrongylus colubriformis* (*T. colubriformis*) are common parasitic nematodes of ruminants and responsible for major economic losses on farms worldwide.[1e] *H. contortus* is located in the abomasum (stomach) of the host where it feeds on blood, whereas *T. colubriformis* affects the anterior small intestine.[1e] Since these species can co-exist in similar climatic regions and co-infect animals, it is desirable to have anthelmintics that efficiently kill both parasites.[1e] Here, all organic precursors and organometallic analogues of monepantel were screened for their activities against these two parasites in a larval development assay (LDA) (see SI for details) and the results are summarized in Tables 1 and 2.

Table 1. Activity of organic intermediates **3a-3n** against *Haemonchus contortus* and *Trichostrongylus colubriformis* in a larval development assay (LDA) and against *Dirofilaria immitis* microfilariae *in v*itro ([a]EC_{100} value;[5] n.d.i. = non-disclosable information[25]). EC values are given in µg/mL as well as in µM.

Compound	EC_{60} value				EC_{50} value			
	H. contortus		*T. colubriformis*		*D.immitis* 24 hours		*D.immitis* 48 hours	
	[µg/mL]	[µM]	[µg/mL]	[µM]	[µg/mL]	[µM]	[µg/mL]	[µM]
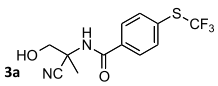 **3a**	9.50	31.20	>10.00	>32.90	>10.00	>32.90	0.49	1.61
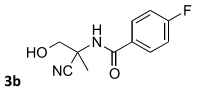 **3b**	>10.00	>45.00	>10.00	>45.00	>10.00	>45.00	>10.00	>45.00
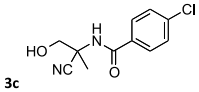 **3c**	>10.00	>41.90	>10.00	>41.90	>10.00	>41.90	6.60	27.65
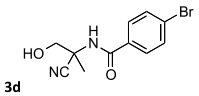 **3d**	>10.00	>35.32	>10.00	>35.32	>10.00	>35.32	>10.00	>35.32
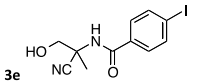 **3e**	>10.00	>30.29	>10.00	>30.29	>10.00	>30.29	>10.00	>30.29
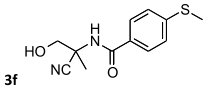 **3f**	>10.00	>39.94	>10.00	>39.94	>10.00	>39.94	>10.00	>39.94
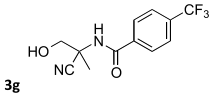 **3g**	>10.00	>36.73	>10.00	>36.73	>10.00	>36.73	>10.00	>36.73
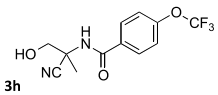 **3h**	>10.00	>34.70	6.60	22.89	>10.00	>34.70	>10.00	>34.70
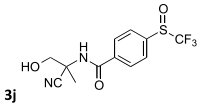 **3j**	>10.00	>31.22	>10.00	>31.22	>10.00	>31.22	6.60	20.61
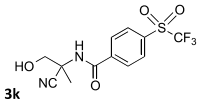 **3k**	>10.00	>29.74	>10.00	>29.74	>10.00	>29.74	>10.00	>29.74
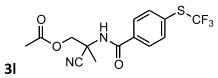 **3l**	3.00	8.66	4.00	11.55	>10.00	>28.88	6.60	19.06
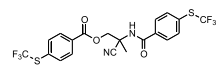 **3m**	>10.00	>19.67	>10.00	>19.67	>10.00	>19.67	6.60	12.98
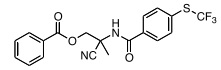 **3n**	4.20	10.28	5.80	14.20	>10.00	>24.49	>10.00	>24.49
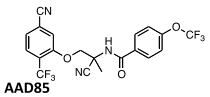 **AAD85**	0.01[a]	0.022[a]	0.032[a]	0.07[a]	2.40	5.25	2.20	4.81
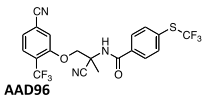 **AAD96**	0.01[a]	0.021[a]	0.032[a]	0.07[a]	n.d.i.	n.d.i.	n.d.i.	n.d.i.
Ivermectin	0.001[a]	0.001[a]	0.01[a]	0.001[a]	1.00 - 3.00	1.14-3.43	1.00 - 3.00	1.14-3.43

Table 2. Activity of organometallic analogues of monepantel **5a-5h, 7a, 7b, 9a** and **9b** against *Haemonchus contortus* and *Trichostrongylus colubriformis* in a larval development assay (LDA) and against *Dirofilaria immitis* microfilariae *in v*itro ([a]EC_{100} value[5]; n.d.i. = non-disclosable information[25]). EC values are given in µg/mL as well as in µM.

Compound	EC_{60} value				EC_{50} value			
	H. contortus		*T. colubriformis*		*D.immitis* 24 hours		*D.immitis* 48 hours	
	[µg/mL]	(µM)	[µg/mL]	(µM)	[µg/mL]	(µM)	[µg/mL]	(µM)
5a 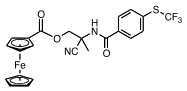	2.10	4.07	6.30	12.20	>10.00	>19.37	>10.00	>19.37
5b 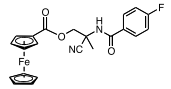	>10.00	>23.03	>10.00	>23.03	>10.00	>23.03	6.60	15.20
5c 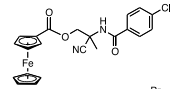	>10.00	>22.19	>10.00	>22.19	>10.00	>22.19	6.60	14.64
5d 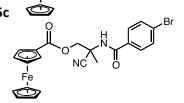	>10.00	>20.20	>10.00	>20.20	>10.00	>20.20	4.20	8.48
5e 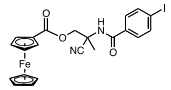	4.50	8.30	>10.00	>18.45	>10.00	>18.45	6.60	12.17
5f 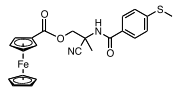	>10.00	>21.63	>10.00	>21.63	>10.00	>21.63	>10.00	>21.63
5g 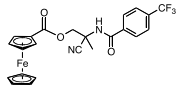	>10.00	>20.65	>10.00	>20.65	>10.00	>20.65	6.60	13.63
5h 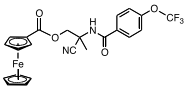	3.00	6.00	7.00	14.00	>10.00	>20.00	>10.00	>20.00
5j 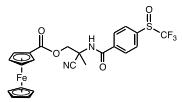	>10.00	>18.79	>10.00	>18.79	>10.00	>18.79	>10.00	>18.79
5k 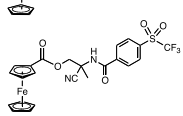	1.80	3.30	4.60	8.40	>10.00	>18.24	>10.00	>18.24
7a 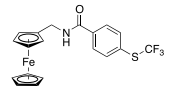	6.00	14.31	8.30	19.79	2.00	5.25	2.10	5.10
7b 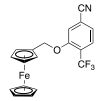	>10.00	>26.00	>10.00	>26.00	>10.00	>26.00	>10.00	>26.00
9a 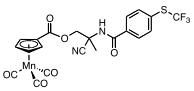	>10.00	>18.71	>10.00	>18.71	>10.00	>18.71	1.80	3.37
9b 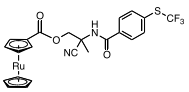	>10.00	>17.80	>10.00	>17.80	>10.00	>17.80	>10.00	>17.8
AAD85 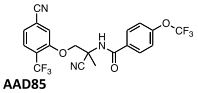	0.01[a]	0.022[a]	0.032[a]	0.07[a]	2.40	5.25	2.20	4.81
AAD96 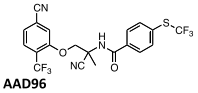	0.01[a]	0.021[a]	0.032[a]	0.07[a]	n.d.i.	n.d.i.	n.d.i.	n.d.i.
Ivermectin	0.001[a]	0.001[a]	0.01[a]	0.001[a]	1.00 - 3.00	1.14-3.43	1.00 - 3.00	1.14-3.43

At the highest concentration tested (10 μg/mL), 9 of the 27 compounds showed moderate activities against *H. contortus* and *T. colubriformis,* with EC_{60} values ranging from 1.80-9.50 μg/mL (3.30-31.20 μM). The potencies of our compounds were lower than that of the parent compound monepantel against *H. contortus* and *T. colubriformis*.[5] Most of the organic intermediates **3a-3k** were not active. However, the insertion of the ferrocenyl moiety generally increased activity, as observed for compounds **5a**, **5e**, **5h** and **5k**. Specifically, **3a**, the organic precursor of **5a**, had EC_{60} values of 9.50 μg/mL (31.20 μM) and >10.00 μg/mL (>32.90 μM) against *H. contortus* and *T. colubriformis*, respectively; by contrast, **5a** displayed EC_{60} values of 2.10 μg/mL (4.07 μM) and 6.30 μg/mL (12.20 μM), respectively. Within the series of halides containing organometallic compounds (**5b-5e**), **5e**, with an iodide, displayed an EC_{60} of 4.5 μg/mL (8.30 μM) on *H. contortus*. However, this compound was inactive (>10 μg/mL/ >18.45 μM) on *T. colubriformis*; **5e** was the only analogue shown to be active on *H. contortus* but not on *T. colubriformis*.

An exchange of the SCF_3 group in **5a** with an OCF_3 group in **5h** led to a slight decrease in activity against both parasites (EC_{60} increased by 43% for *H. contortus* and by 11% for *T. colubriformis*). Oxidizing the SCF_3 group of **5a** to its sulfone in **5k** increased the activity slightly (EC_{60} decrease of 14% for *H. contortus* and 27% for *T. colubriformis*). However, the sulfoxide **5j** had no activity using the highest concentration tested (10 μg/mL/ >18.79 μM). Overall, the order of potencies with substitutions at the benzamide unit of the active analogues of **5a** is $S(O)_2CF_3 \geq SCF_3 \geq OCF_3 > I$.

A replacement of the ferrocenyl moiety of **5a** with a cymantrenyl and ruthenocenyl unit in **9a** and **9b**, respectively, rendered the compound inactive against *H. contortus* and *T. colubriformis*. The inactivity of **9b**, in particular, suggests that **5a** may have a partial, metal-coupled mode of action. Based on previous biological studies on ferrocenyl and ruthenocenyl derivatives,[11b, 16b, 19a, 26] it seems reasonable to speculate that the ferrocene moiety of **5a,** but not the ruthenocene moiety in **9b**, can cause ROS generation inside the parasite, and that this ROS is at least partly responsible for the activity of **5a**. Indeed, we found that ROS generation by **5a** is significantly higher than **9b,** as described below.

Potentiation of ion channel current

The ferrocenyl compound **5a** was more efficacious against *H. contortus* and *T. colubriformis* than its organic counterpart **3a**. This difference might arise from the ability of the ferrocenyl compound to potentiate the ion channels better than the organic counterpart. Alternatively, the presence of the hydrophobic ferrocenyl entity in **5a** might enhance the accumulation of the compound in the worm's tissues, or impart a secondary function, such as ROS production. To test whether a better potentiation of ion channel currents contributed to the increased efficacy of **5a**, we compared the ability of compounds **3a**, **3l**, and **5a** to potentiate the monepantel target ACR-23 of *C. elegans* expressed in oocytes of *Xenopus laevis*. Monepantel acts as a positive allosteric modulator, increasing ion channel current when it is co-applied with an agonist.[6a, 6c, 7] To quantify the potentiation of this channel by our compounds, we co-applied them with the agonist betaine (300 μM, ~EC_{15} concentration) and compared the current with control recordings using betaine alone.

All three compounds showed decent efficacies in this assay. The least potent and efficacious compound was **3l**, with an EC_{50} of 9 μM and maximal potentiation of 9-fold compared with the current induced by betaine alone. The potency and efficacy of compounds **3a** and **5a** were similar; **3a** had an EC_{50} of 2.1 μM, with maximal potentiation of 30-fold, and **5a** had an EC_{50} of 1.2 μM, with maximal potentiation of 32-fold (Figure 3). The less than 2-fold difference in EC_{50} value between these two compounds is negligible, and seems to result mostly from a considerable difference in the slope of the response curves (Hill coefficient = 2.1 for **3a** and 11.5 for **5a**). The steep slope of the curve for **5a** could be caused by limited aqueous solubility, affecting the measurements at higher concentrations.

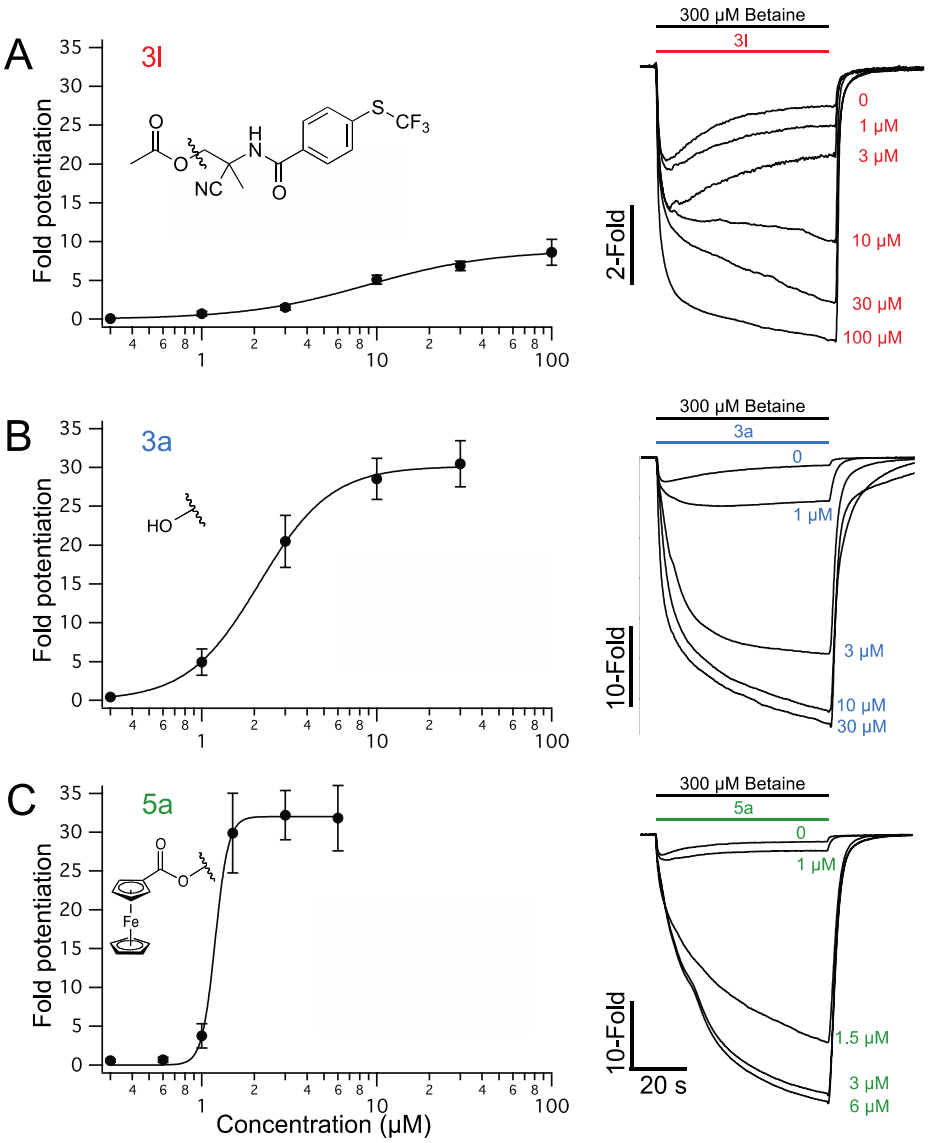

Figure 3. Potentiation of ACR-23 channels expressed in *Xenopus laevis* oocytes sustained co-application with 300 μM betaine. (A) compound **3l**. (B) compound **3a**. (C) compound **5a**. *left*, concentration-response curves. Insets indicate the chemical groups that are different between the three compounds. Fold potentiation represents the current after 1 minute of sustained co-application with betaine, normalized to the current from applying betaine alone. n = 5-8 recordings from independent oocytes. Error bars are SEM. *Right*, representative current traces from co-application of AAD compounds with the agonist betaine.

The efficacy of these three compounds potentiating ACR-23 channels follows the order **5a** ≈ **3a** > **3l**. This efficacy differs from that against *H. contortus* and *T.*

colubriformis, which follows the order **5a** ≈ **3l** > **3a**. The marked efficacy of **3a**, when assayed on the ion channel, demonstrates that the ferrocenyl group of **5a** and the corresponding aryloxy group of monepantel are not essential for receptor potentiation. Therefore, the aryloxy group of monepantel is likely to contribute to favorable pharmacokinetic properties or pharmacological potency, rather than efficacy. The ferrocenyl group of **5a** either partially recapitulates these properties, or confers novel toxic properties. These results are consistent with the differences in anti-parasitic activity of compounds **5a** and **9b**, indicating that redox-mediated toxic properties of ferrocene might contribute to the toxicity of **5a**.

Production of ROS

The rationale behind the design of our organometallic-containing monepantel derivatives was the introduction of metal-specific modes of action into the organic drug. For example, we envisaged that the redox properties of the ferrocene/ferrocenium system in **5a** might lead to the production of toxic ROS and thus improve anti-parasitic activity of the organic drug.[27] As discussed earlier, **5a** exhibited moderate activity against *H. contortus* and *T. colubriformis*, but the ruthenocenyl analogue, **9b**, is inactive. To confirm that our compounds have the predicted redox properties, we assessed ROS induced by selected compounds (**3a**, **5a**, **9a** and **9b**) in living cells. Although it would have been ideal to investigate ROS production in parasites, for practical and technical reasons, we used a mammalian cervical cancer cell line (HeLa). To do this, cells were treated with different compounds (25 μM for 20 h), and the intracellular ROS was quantified using the oxidation-sensitive fluorescent indicator 2′,7′-dichlorofluorescein diacetate (H2DCFDA); *tert*-Butyl hydroperoxide (TBH) was employed as a positive control (100 μM for 6 h). The ROS level in cells treated with **3a** was similar to that of the untreated control cells. By contrast, compound **5a**, which results from the attachment of a ferrocenyl moiety to **3a**, produced 2.4-fold higher level of ROS than the organic precursor (**3a**) alone. ROS induced by the ruthenocene analogue **9b** was significantly ($P < 0.001$) lower than for **5a**. This difference in ROS production might be one of the factors responsible for the difference in potency between **5a** and **9b** against *H. contortus* and *T. colubriformis* (Figure 4). Additionally, we evaluated ROS production

following exposure to the cymantrene analogue **9a**. The ROS level induced by **9a** were comparable to its organic precursor (**3a**).

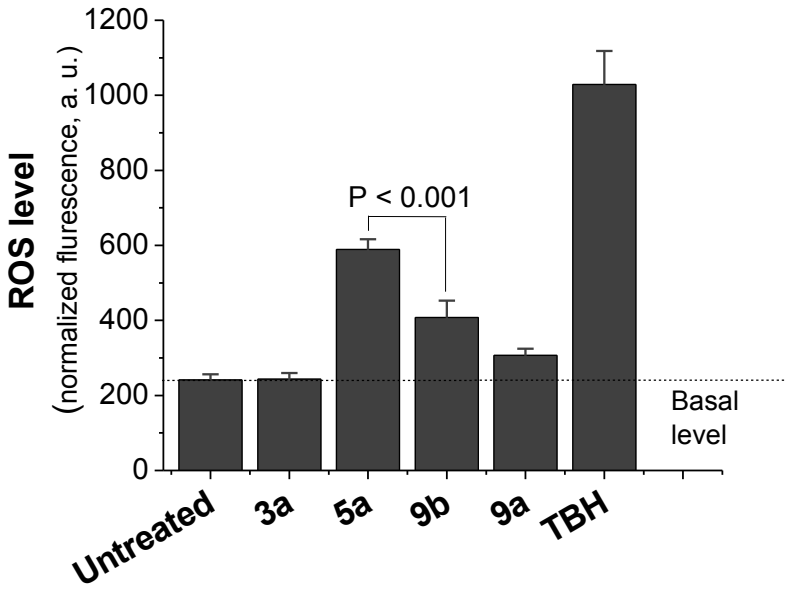

Figure 4. Level of ROS in HeLa cells treated with **3a**, **5a**, **9a** and **9b**. TBH: *tert*-butyl hydroperoxide.

Activity against filarial nematodes

As organometallic derivatization was shown previously to modulate the activity profiles of organic drugs,[11b, 16b, 26] we assayed the activity of our new class of anthelmintics against other parasites. We were eager to assess the activity of our compounds on taxonomically and biologically disparate groups of parasites, including *D. immitis* (canine heartworm), *Ctenocephalides felis* (*C. felis*, cat flea), *Lucilia cuprina* (*L. cuprina*, blow fly) and *Rhipicephalus sanguineus* (*R. sanguineus*, brown dog tick). Neither AAD85 nor the compounds synthesized in this study had activity (at the highest concentration tested) on *C. felis* (100 μg/mL), *L. cuprina* (32 μg/mL) or *R. sanguineus* (100 μg/mL and 640 μg/mL) (Table S4). Compound **5a**, and four other compounds effective against *H. contortus* and *T. colubriformis* in a larval development assay (LDA) (**3h**, **3n**, **5h**, and **5k**), displayed no activity against *D. immitis* in a motility assay. However, 12 out of 27 compounds displayed considerable activity against *D. immitis* microfilariae, in a similar range as the standard heartworm treatment agent ivermectin.[28] The organic precursor, **3a**, was extremely active

against this parasite, with an EC_{50} value of 0.49 μg/mL (1.61 μM) after 48 h. Other organic precursors (**3c**, **3j**, **3l** and **3m**) had lower activities, with EC_{50} values of 6.60 μg/mL (12.98-27.65 μM). The activities of organometallic derivatives were moderate; **5b**, **5c**, **5d, 5e**, **5g** and **7a** displayed EC_{50} values of 2.00-6.60 μg/mL (5.10-15.20 μM). Interestingly, the organometallic analogue, **7a**, bearing only the benzamide unit and lacking the C2 spacer was the only compound that was active against all three parasitic nematodes tested (i.e. *H. contortus*, *T. colubriformis* and *D. immitis*); **7a** is also the only compound that displayed activity after only 24 h. The replacement of ferrocene in **5a** with a cymantrene unit makes the resultant analogue, **9a**, active against *D. immitis*, with an EC_{50} value of 1.80 μg/mL (3.37 μM).

Because AAD activity against filarial nematodes has not been reported previously, we decided to also test a close analog of monepantel, AAD85. This compound has activity similar to that of compound **7a**; it is less potent than **3a**, but acts within 24 h. The *D. immitis* genome does not appear to encode a close homolog of the receptors targeted by monepantel, suggesting that this species has a novel AAD target. This proposal is supported by the lack of activity against *D. immitis versus* efficacy against other species.[29] Moreover, there is no correlation between ROS production and activity against *D. immitis*, indicating a non-specific effect of ROS.

Cytotoxicity and Stability of 3a and 9a

An ideal anti-parasitic compound should be selective in killing worms while being non-toxic to the mammalian host. We evaluated the selectivity of the two most active compounds against *D. immitis*, **3a** and **9a**. We determined their cytotoxicity using non-cancerous human embryonic kidney (HEK293) cells. The metal-based anticancer drug cisplatin was used as positive control. Cisplatin inhibits the growth of HEK293 cells at an IC_{50} value 39.62±2.61 μM. Encouragingly, both of the compounds **3a** and **9a** were non-toxic up to 100 μM (the highest concentration assayed), demonstrating selectivity of the compounds towards parasites.

Another important parameter is the stability of the drug candidate. The stabilities of **3a** and **9a** were evaluated by ^{1}H NMR spectroscopy. Compounds were dissolved in a d_6-DMSO/D_2O mixture (1/4 (**3a**); 2/3 (**9a**), v/v) and kept in the dark at room temperature. ^{1}H NMR spectra were recorded at different time intervals. No

decomposition of the compounds was observed after a 48 h incubation time, confirming the stability of **3a** and **9a** in aqueous media (see Figure S4 and S5).

Conclusion

Given the emergence of drug resistance in some socioeconomically important parasitic nematodes, new strategies are needed to discover drugs with novel modes of action. In this study, we explored metal-based variants to "expand the chemical space" for anti-parasitic drug candidates. Starting from the organic drug monepantel as a lead structure, we designed and synthesized a series of organic and organometallic analogues employing two different strategies. The efficacies of the structurally diverse organometallic analogues as well as various organic intermediates were evaluated against *H. contortus* and *T. colubriformis*. Compounds **3a**, **3h**, **3l**, **3n**, **5a**, **5e**, **5h**, **5k** and **7a** showed moderate activity against these two nematodes. Further biological assessments on other parasites revealed that 11 of our new compounds had activity against *D. immitis* microfilariae (low µg/mL range) for three compounds (**3a**, **9a** and **7a**). Among these three most active compounds, **7a** is the unique candidate showing anti-parasitic activity against all three parasitic nematodes. However, no clear structure-activity relationship in efficacy of our compounds between *H. contortus/T. colubriformis* and *D. immitis* could be found, suggesting a unique mechanism of action for the compounds in the canine heartworm.

Experimental section

Synthesis and characterization of organic precursors (**3a-3g, 3j-3n**) and organometallic analogues (**5a-5k**, **7a**, **7b**, **9a**, **9b**) can be found in the supporting information.

Supporting information

General remarks (materials, instrumentation and methods, X-ray crystallography, cell culture, cytotoxicity studies, ROS generation, biological assays, electrophysiology methods), synthesis and characterization of **3a-3n**, **5b-5k**, **7a**, **7b**, **8c**, **9a**, **9b**, NMR spectra of compounds, Figure S1-S3 (Molecular structures of **3a, 3b, 3g, 5c, 5h, 5a** and **5k)**, Table S1 (Crystal data and structure refinement for **3a**, **3b**, **3f**, and **3g**), Table

S2 (Crystal data and structure refinement for **5a, 5c** and **5d**). Table S3 (Crystal data and structure refinement for **5h** and **5k**), Table S4 (Anti-parasitic activity against *Ctenocephalides felis*, *Lucilia cuprina* and *Rhipicephalus sanguineus* of organometallic derivatives **3a-3n**), Table S5 (Anti-parasitic activity against *Ctenocephalides felis*, *Lucilia cuprina* and *Rhipicephalus sanguineus* of organometallic derivatives **5a-5k, 7a**, **7b**, **9a, 9b**), Figure S4-S5 (^{1}H NMR spectra of **3a** and **9a** in different time intervals).

Acknowledgements

This work was financially supported by the Swiss National Science Foundation (Professorships N° PP00P2_133568 and PP00P2_157545to G.G), the University of Zurich (G.G), the Stiftung für wissenschaftliche Forschung of the University of Zurich (G.G), the Novartis Jubilee Foundation (G.G) and the Swiss Government Excellence Scholarship for Postdoctoral Researcher (R.L.). R.B.G.'s research program is supported by the Australian Research Council (ARC), the National Health and Medical Research Council (NHMRC), Wellcome Trust, Melbourne Water Corporation, Yourgene Bioscience, the Alexander von Humboldt Foundation and The University of Melbourne. E.M.J. is supported by the US National Institutes of Health (NINDS R01-NS034307) and is an Investigator of the Howard Hughes Medical Institute (HHMI). R.B.G. and E.M.J. are grateful recipients of Professorial Humboldt Research Awards. The authors would like to thank Dr. Jacques Bouvier (Novartis Animal Health, St-Aubin, Switzerland) and Dr. Noëlle Gauvry (Novartis Animal Health, Basel, Switzerland) for their help with the biological assays.

Keywords: Anti-parasitic compounds • bioorganometallic chemistry • *D. immitis* • *H. contortus* • livestock industry • medicinal chemistry • monepantel.

References

[1] a). Otranto, R. Wall, *Med. Vet. Entomol.* **2008**, *22*, 291-302; b). D. Sargison, *Vet. Parasitol.* **2012**, *189*, 79-84; c). K. Grencis, *Annu. Rev. Immunol.* **2015**, *33*, 201-225; d). Traversa, *Parasit. Vectors* **2012**, *5*, 91-91; e). Roeber, A. Jex, R. Gasser, *Parasit Vectors* **2013**, *6*, 153; f). Kaminsky, L. Rufener, J. Bouvier, R. Lizundia, S. Schorderet Weber, H. Sager, *Vet. Parasitol.* **2013**, *195*, 286-291; g). R. Sykes, *Anim. Sci.* **1994**, *59*, 155-172.

[2] a). Holden-Dye, R. J. Walker, *Anthelmintic drugs*, The C.elegans Research Community ed., WormBook, **2007**; b). Epe, R. Kaminsky, *Trends Parasitol.* **2013**, *29*, 129-134; c). E. Campbell, M. Tarleton, C. P. Gordon, J. A. Sakoff, J. Gilbert, A. McCluskey, R. B. Gasser, *Bioorg. Med. Chem. Lett.* **2011**, *21*, 3277-3281; d). L. Blagburn, M. W. Dryden, *Vet. Clin. North Am. Small Anim. Pract.* **2009**, *39*, 1173-1200.

[3] a). M. Kaplan, A. N. Vidyashankar, *Vet. Parasitol.* **2012**, *186*, 70-78; b). A. Sutherland, D. M. Leathwick, *Trends Parasitol.* **2011**, *27*, 176-181; c). J. Wolstenholme, I. Fairweather, R. K. Prichard, G. von Samson-Himmelstjerna, N. C. Sangster, *Trends Parasitol.* **2004**, *20*, 469-476; d). Van den Brom, L. Moll, C. Kappert, P. Vellema, *Vet. Parasitol.* **2015**, *209*, 278-280; e). Mederos, Z. Ramos, G. Banchero, *Parasit Vectors* **2014**, *7*, 598; f). S. Cezar, G. Toscan, G. Camillo, L. A. Sangioni, H. O. Ribas, F. S. F. Vogel, *Vet. Parasitol.* **2010**, *173*, 157-160; g). Coles, M. Dryden, *Parasit Vectors* **2014**, *7*, 8.

[4] R. Kaminsky, P. Ducray, M. Jung, R. Clover, L. Rufener, J. Bouvier, S. S. Weber, A. Wenger, S. Wieland-Berghausen, T. Goebel, N. Gauvry, F. Pautrat, T. Skripsky, O. Froelich, C. Komoin-Oka, B. Westlund, A. Sluder, P. Maser, *Nature* **2008**, *452*, 176-180.

[5] P. Ducray, N. Gauvry, F. Pautrat, T. Goebel, J. Fruechtel, Y. Desaules, S. S. Weber, J. Bouvier, T. Wagner, O. Froelich, R. Kaminsky, *Bioorg. Med. Chem. Lett.* **2008**, *18*, 2935-2938.

[6] a). Rufener, J. Keiser, R. Kaminsky, P. Mäser, D. Nilsson, *PLoS Pathog.* **2010**, *6*, e1001091; b). Rufener, N. Bedoni, R. Baur, S. Rey, D. A. Glauser, J. Bouvier, R. Beech, E. Sigel, A. Puoti, *PLoS Pathog* **2013**, *9*, e1003524; c). S. Peden, P. Mac, Y.-J. Fei, C. Castro, G. Jiang, K. J. Murfitt, E. A. Miska, J. L. Griffin, V. Ganapathy, E. M. Jorgensen, *Nat. Neurosci.* **2013**, *16*, 1794-1801.

[7] R. Baur, R. Beech, E. Sigel, L. Rufener, *Mol Pharmacol* **2015**, *87*, 96-102.

[8] I. Scott, W. E. Pomroy, P. R. Kenyon, G. Smith, B. Adlington, A. Moss, *Vet. Parasitol.* **2013**, *198*, 166-171.

[9] a). Alessio, Wiley-VCH Verlag, Weinheim, **2011**; b). C. Dabrowiak, *Metals in Medicine*, John Wiley & Sons Ltd, Chichester, **2009**; c). Patra, G. Gasser, *ChemBioChem* **2012**, *13*, 1232 – 1252.

[10] a). J. Farrer, P. J. Sadler, in *Bioinorganic Medicinal Chemistry*, Wiley-VCH Verlag GmbH & Co. KGaA, **2011**, pp. 1-47; b). C. A. Bruijnincx, P. J. Sadler, *Curr. Opin. Chem. Biol.* **2008**, *12*, 197-206; c). G. Hartinger, N. Metzler-Nolte, P. J. Dyson, *Organometallics* **2012**, *31*, 5677–5685.

[11] a). Biot, G. Glorian, L. A. Maciejewski, J. S. Brocard, O. Domarle, G. Blampain, P. Millet, A. J. Georges, H. Abessolo, D. Dive, J. Lebibi, *J. Med. Chem.* **1997**, *40*, 3715-3718; b). Dubar, T. J. Egan, B. Pradines, D. Kuter, K. K. Ncokazi, D. Forge, J.-F. o. Paul, C. Pierrot, H. Kalamou, J. Khalife, E. Buisine, C. Rogier, H. Vezin, I. Forfar, C. Slomianny, X. Trivelli, S.

Kapishnikov, L. Leiserowitz, D. Dive, C. Biot, *ACS Chem. Biol.* **2011**, *6*, 275-287.

[12] a). A. Sanchez-Delgado, A. Anzellotti, *Mini Rev. Med. Chem.* **2004**, *4*, 23-30; b). Martinez, T. Carreon, E. Iniguez, A. Anzellotti, A. Sanchez, M. Tyan, A. Sattler, L. Herrera, R. A. Maldonado, R. A. Sanchez-Delgado, *J. Med. Chem* **2012**, *55*, 3867-3877; c). Otero, G. Aguirre, L. Boiani, A. Denicola, C. Rigol, C. Olea-Azar, J. D. Maya, A. Morello, M. Gonz·lez, D. Gambino, H. Cerecetto, *Eur. J. Med. Chem.* **2006**, *41*, 1231-1239; d). R. Maldonado, C. Marin, F. Olmo, O. Huertas, M. Quiros, M. Sanchez-Moreno, M. J. Rosales, J. M. Salas, *J. Med. Chem.* **2010**, *53*, 6964-6972; e). Navarro, E. J. Cisneros-Fajardo, T. Lehmann, R. A. Sanchez-Delgado, R. Atencio, P. Silva, R. Lira, J. A. Urbina, *Inorg. Chem.* **2001**, *40*, 6879-6884; f). A. Sanchez-Delgado, M. Navarro, K. Lazardi, R. Atencio, M. Capparelli, F. Vargas, J. A. Urbina, A. Bouillez, A. F. Noels, D. Masi, *Inorg. Chim. Acta* **1998**, *275-276*, 528-540; g). A. Sanchez-Delgado, K. Lazardi, L. Rincon, J. A. Urbina, A. J. Hubert, A. N. Noels, *J. Med. Chem.* **1993**, *36*, 2041-2043; h). Navarro, T. Lehmann, E. J. Cisneros-Fajardo, A. Fuentes, R. A. Sanchez-Delgado, P. Silva, J. A. Urbina, *Polyhedron* **2000**, *19*, 2319-2325; i). J. N. Silva, P. M. M. Guedes, A. Zottis, T. L. Balliano, F. O. Nascimento Silva, L. G. França Lopes, J. Ellena, G. Oliva, A. D. Andricopulo, D. W. Franco, J. S. Silva, *Br. J. Pharmacol.* **2010**, *160*, 260-269; j). Iniguez, A. Sanchez, M. Vasquez, A. Martinez, J. Olivas, A. Sattler, R. Sanchez-Delgado, R. Maldonado, *J. Biol. Inorg. Chem.* **2013**, *18*, 779-790; k). Navarro, C. Gabbiani, L. Messori, D. Gambino, *Drug Discov. Today* **2012**, *15*, 1070-1078.

[13] M. Patra, G. Gasser, N. Metzler-Nolte, *Dalton Trans.* **2012**, *41*, 6350-6358.

[14] a). Hess, J. Keiser, G. Gasser, *Future Med. Chem* **2015**, *7*, 821-830; b). Patra, K. Ingram, A. Leonidova, V. Pierroz, S. Ferrari, M. N. Robertson, M. H. Todd, J. Keiser, G. Gasser, *J. Med. Chem.* **2013**, *56*, 9192-9198; c). Patra, K. Ingram, V. Pierroz, S. Ferrari, B. Spingler, R. B. Gasser, J. Keiser, G. Gasser, *Chem. Eur. J.* **2013**, *19*, 2232-2235; d). Patra, K. Ingram, V. Pierroz, S. Ferrari, B. Spingler, J. Keiser, G. Gasser, *J. Med. Chem.* **2012**, *55*, 8790-8798.

[15] a). Gasser, N. Metzler-Nolte, *Curr. Opin. Chem. Biol.* **2012**, *16*, 84-91; b). Gasser, I. Ott, N. Metzler-Nolte, *J. Med. Chem.* **2011**, *54*, 3-25; c). Jaouen, N. Metzler-Nolte, in *Topics in Organometallic Chemistry, Vol. 32; and references therein*, 1st ed., Springer, Heidelberg, Germany, **2010**; d). Hartinger, P. J. Dyson, *Chem. Soc. Rev.* **2009**, *38*, 391-401; e). C. A. Bruijnincx, P. J. Sadler, *Curr. Opin. Chem. Biol.* **2008**, *12*, 197-206, and references therein; f). Biot, G. Glorian, L. A. Maciejewski, J. Brocard, *J. Med. Chem.* **1997**, *40*, 3715-3718; g). Biot, D. Dive, in *Medicinal Organometallic Chemistry, Vol. 32* (Eds.: G. Jaouen, N. Metzler-Nolte), Springer-Verlag, Heidelberg, **2010**, pp. 155-193; h). Biot, W. Castro, C. Y. Botte, M. Navarro, *Dalton Trans.* **2012**, *41*, 6335-6349; i). Dive, C. Biot, *ChemMedChem* **2008**, *3*, 383 - 391.

[16] a). Dallagi, M. Saidi, A. Vessières, M. Huché, G. Jaouen, S. Top, *J. Org. Chem.* **2013**, *734*, 69-77; b). Jaouen, S. Top, A. Vessières, G. Leclercq, M. J. McGlinchey, *Curr. Med. Chem.* **2004**, *11*, 2505-2517; c). Top, A. Vessières, G. Leclercq, J. Quivy, J. Tang, J. Vaissermann, M. Huché, G. Jaouen, *Chem. Eur. J.* **2003**, *9*, 5223-5236.

[17] P. M. Loiseau, J. J. Jaffe, D. G. Craciunescu, *Int. J. Parasitol.* **1998**, *28*, 1279-1282.

[18] a). Lifschitz, M. Ballent, G. Virkel, J. Sallovitz, P. Viviani, C. Lanusse, *Vet. Parasitol.* **2014**, *203*, 120-126; b). Stuchlikova, R. Jirasko, I. Vokral, J. Lamka, M. Spulak, M. Holcapek, B. Szotakova, H. Bartikova, M. Pour, L. Skalova, *Anal. Bioanal. Chem.* **2013**, *405*, 1705-1712.

[19] a). Pigeon, S. Top, A. Vessières, M. Huché, E. A. Hillard, E. Salomon, G. Jaouen, *J. Med. Chem.* **2005**, *48*, 2814-2821; b). Chavain, H. Vezin, D. Dive, N. Touati, J.-F. Paul, E. Buisine, C. Biot, *Mol. Pharmaceutics* **2008**, *5*, 710-716.

[20] a). Glans, W. Hu, C. Jost, C. de Kock, P. J. Smith, M. Haukka, H. Bruhn, U. Schatzschneider, E. Nordlander, *Dalton Trans.* **2012**, *41*, 6443-6450; b). V. Simpson, C. Nagel, H. Bruhn, U. Schatzschneider, *Organometallics* **2015**, *34*, 3809-3815.

[21] P. Ducray, N. Gauvry, T. Goebel, M. Jung, R. Kaminsky, F. Pautrat, (Ed.: WO/2005/044784), Google Patents, **2005**.

[22] D. Karadzovska, W. Seewald, A. Browning, M. Smal, J. Bouvier, J. M. Giraudel, *J. Vet. Pharmacol. Therap.* **2009**, *32*, 359-367.

[23] a). R. Biehl, P. C. Reeves, *Synthesis* **1973**, *1973*, 360-361; b). P. Cormode, A. J. Evans, J. J. Davis, P. D. Beer, *Dalton Trans.* **2010**, *39*, 6532-6541.

[24] a). D. Beer, D. K. Smith, *J. Chem. Soc., Dalton Trans.* **1998**, 417-424; b). G. Hardy, L. Ren, T. C. Tamboue, C. Tang, *J. Polym. Sci., Part A: Polym. Chem.* **2011**, *49*, 1409-1420.

[25] For legal issues the efficacy of AAD96 cannot be disclosed.

[26] C. Biot, W. Daher, N. Chavain, T. Fandeur, J. Khalife, D. Dive, E. De Clercq, *J. Med. Chem.* **2006**, *49*, 2845-2849.

[27] R. Rubbiani, O. Blacque, G. Gasser, *Dalton Trans.* **2016**.

[28] D. D. Bowman, C. Mannella, *Top. Companion Anim. Med.* **2011**, *26*, 160-172.

[29] C. Godel, S. Kumar, G. Koutsovoulos, P. Ludin, D. Nilsson, F. Comandatore, N. Wrobel, M. Thompson, C. D. Schmid, S. Goto, F. Bringaud, A. Wolstenholme, C. Bandi, C. Epe, R. Kaminsky, M. Blaxter, P. Mäser, *FASEB J.* **2012**, *26*, 4650-4661.

Table of content

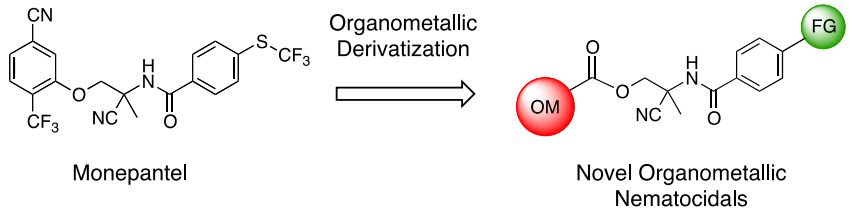

Monepantel

Novel Organometallic Nematocidals

We report the synthesis and biological evaluation of organometallic compounds, based on the lead structure of monepantel, and remarkable activity against some economically important parasitic worms of animals.